RASĀYAN *J. Chem.*
Vol. 19 | No. 2 | 858-865| April-June | 2026
ISSN: 0974-1496 | e-ISSN: 0976-0083 | CODEN: RJCABP
http://www.rasayanjournal.com
http://www.rasayanjournal.co.in

OCTAHEDRAL TRANSITION METAL COMPLEXES OF HBMTAAP WITH ENHANCED ANTIMICROBIAL ACTIVITY AND LIGAND-BASED *PFDHFR* DOCKING STUDY

D. B. Zarekar[1]✉, G. S. Jha[2], R. R. Badekar[3], R. G. Gupta[3] and S. V. Jaybhaye[1]
[1]Department of Chemistry, B. K. Birla College (Empowered Autonomous Status), Kalyan-421301, (Maharashtra), India
[2]Platinum Industries Limited, Palghar-401404, (Maharashtra), India
[3]Riva Industries, 289/ Kirwali, Raigad-410201, (Maharashtra), India
✉Corresponding author: dzarekar11@gmail.com

ABSTRACT
A novel thiocarbohydrazide-derived Schiff base ligand, α-benzilmonoximethiocarbohydrazide-4′-aminoacetophenone (HBMTAAP), was synthesized and coordinated with first-row transition metal ions to form ML_2 complexes. Spectral and magnetic data confirmed that all complexes are neutral and non-electrolytic with octahedral geometry, except for Cu(II), which exhibits Jahn–Teller–induced tetragonal distortion. Antibacterial and antifungal tests showed moderate activity for the free ligand, with enhanced inhibition observed upon metal coordination, especially for the Zn(II), Ni(II), and Cu(II) complexes. Molecular docking with *Plasmodium falciparum dihydrofolate reductase* (1VDR) indicated that HBMTAAP binds strongly (–9.2 kcal/mol), surpassing Proguanil and approaching the binding affinity of Atovaquone. These results demonstrate the potential of HBMTAAP-based metal complexes for promising antibacterial and antimalarial applications, advancing medicinal inorganic chemistry, will supporting Sustainable Development of good health and well-being.
Keywords: Schiff Base, *Plasmodium Falciparum Dihydrofolate Reductase* (*PfDHFR*), HBMTAAP, Transition Metal Complexes, Antimicrobial Activity, Octahedral Geometry.
RASĀYAN *J. Chem.*, Vol. 19, No. 2, 2026

INTRODUCTION

Schiff base ligands continue to attract considerable attention in coordination chemistry because of their diverse binding behaviour and broad biological relevance. Formed through the condensation of primary amines with aldehydes or ketones, these compounds contain the characteristic azomethine (>C=N–) functional group, which serves as an efficient coordination site for transition metal ions.[1] Their ease of synthesis, structural tunability, and strong donor capabilities have made them highly valuable in coordination and bioinorganic chemistry.[2-6] The lone pair of electrons on the azomethine nitrogen facilitates effective coordination, leading to stable metal complexes with diverse geometries and notable physicochemical and biological properties.[7-15] Beyond their structural significance, Schiff base complexes have demonstrated promising biological properties, including antimicrobial, antifungal, antioxidant, anticancer, and antiviral activities.[2-17] The enhancement of biological activity upon metal coordination is frequently explained by chelation theory, where partial sharing of electrons between ligand donor atoms and the metal ion reduces overall polarity and increases lipophilicity.[2-4] This improved lipophilic character facilitates penetration through microbial cell membranes, thereby influencing pharmacological effectiveness. However, thiocarbohydrazide-derived multifunctional ligands containing oxime and hydrazide groups remain comparatively less explored, particularly regarding their combined antimicrobial and antimalarial potential. In addition, systematic evaluation of their interaction with *Plasmodium falciparum dihydrofolate reductase* (*PfDHFR*), a key antimalarial drug target, is limited. In this context, a new O/N/S-donor Schiff base ligand, α-benzilmonoximethiocarbohydrazide-4′-aminoacetophenone (HBMTAAP), was designed and synthesized, followed by coordination with first-row transition metal ions. The resulting complexes were structurally described and assessed for antimicrobial activity, while the ligand was assessed through molecular docking against *PfDHFR*. This integrated investigation aims to

http://doi.org/10.31788/RJC.2026.1929661

correlate structural features with biological performance and supports sustainable development by contributing to the search for new antimicrobial and antimalarial agents.

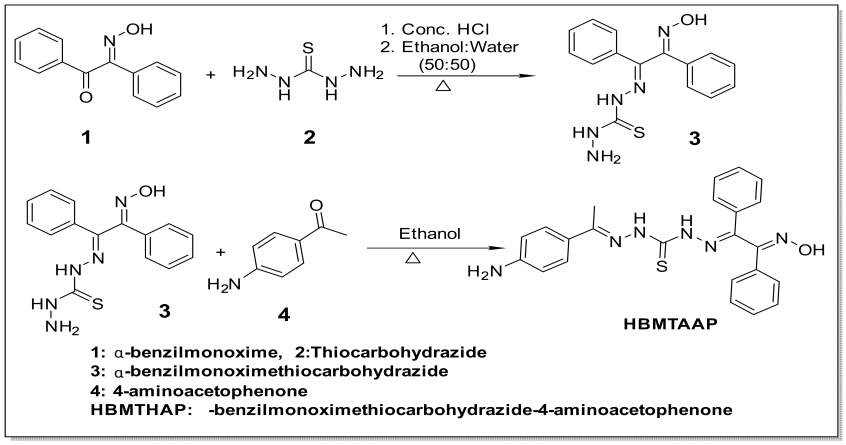

Scheme-1: Synthesis of HBMTAAP Ligand.

EXPERIMENTAL

Materials and Reagents

All the analytical grade reagents were used exactly as supplied. Thiocarbohydrazide, Hydroxylamine hydrochloride, Benzil, 4-aminoacetophenone, $MnCl_2 \cdot 4H_2O$, $FeCl_2$, and $CuCl_2 \cdot 2H_2O$, $CoCl_2 \cdot 6H_2O$ and $NiCl_2 \cdot 6H_2O$, pre-coated silica plates were sourced from Sigma-Aldrich and $ZnCl_2$ from Strem Chemicals. The Glacial CH_3COOH, NaOH (flakes), C_2H_5OH, concentrated HCl, and CH_3OH were supplied by SD Fine Chemicals.

Instruments

The melting temperatures were measured using an Electrothermal 9200 digital melting point device.[2] Spectroscopic characterisation was performed using the Perkin-Elmer Spectrum 100 FT-IR instrument, Perkin-Elmer Lambda 25 UV-Vis spectrophotometer, Rigaku Ultima IV X-ray diffractometer, Bruker AV III 400 MHz NMR spectrometer, and Bruker EVOQ LC-MS system.[2-3] Using a CyberScan CON 510 conductivity meter, molar conductance was determined. Gouy's Method (Model No: HO-ED-EM-08) was used to determine magnetic susceptibility.[38,39] Elemental (CHNS) analysis was performed using a PerkinElmer 2400 analyzer.[4]

Synthesis of the Schiff Base Ligand (HBMTAAP)

The intermediate α-benzilmonoxime was prepared properly according to Vogel and Wazir et al.'s procedures.[20,21] HBMTAAP was then prepared via a two-step, one-pot method (Scheme 1). A mixture of α-benzilmonoxime (22.52 g, 0.100 mol) and thiocarbohydrazide (11.15 g, 0.105 mol) was refluxed in 200 mL of 1:1 (v/v) water–ethanol for 3 h in the presence of 1.8 g HCl as a catalyst.[4] After cooling, the material was collected by filtration, refined by recrystallisation from 60% methanol, and then dried under low pressure to produce a yellow crystalline product.

Molecular Formula$C_{23}H_{22}N_6OS$. **Molecular Weight:** 430.54 g/mol. **Mass Spectrum (LC-MS):** m/z = 431.16 $[M]^+$.

Metal Complexes Synthesis

The ML_2 complexes of HBMTAAP with Mn(II), Fe(II), Co(II), Ni(II), Cu(II), and Zn(II), shown in Scheme 2, were synthesized by reacting a warm ethanolic solution of (0.02 mol) HBMTAAP with the corresponding (0.01 mol) metal chloride solution.[32] By adding aqueous NaOH, the reaction mixture's pH was brought to about 7. Then, the mixture was refluxed for five to ten hours. After cooling, the end product precipitates, then is filtered, rinsed with ethanol, dried, and stored in a desiccator.

Molecular Docking

The molecular docking analysis was conducted using *Plasmodium falciparum dihydrofolate reductase* (*PfDHFR*), for which the crystal structure (PDB ID: 1VDR) was accessed from the RCSB Protein Data

Bank.[36] The Schiff base ligand HBMTAAP (standard antimalarial agents), Proguanil and Atovaquone were constructed in ChemDraw and exported in SDF format. Docking simulations were conducted using the CB-Dock2 server, with the grid box configured to encompass the *PfDHFR* active site.[34-35] The docking poses and corresponding interactions were examined using Discovery Studio Visualizer.

Table-1: Physicochemical Characteristics of the HBMTAAP Ligand and Metal Complex

Compound	Theoretical Mol. Wt.	Yield %	Colour	M.P. (ºC)	Element Content (Observed)					
					M	C	H	N	O	S
HBMTAAP	430.54	81	Yellow	180	-	67.10	5.42	16.29	3.74	7.45
$[Mn(HBMTAAP)_2]$	911.25	63	Brown	195	6.02	63.24	4.85	15.37	3.51	7.01
$[Fe(HBMTAAP)_2]$	912.91	65	Blue	193	6.12	63.17	4.87	15.32	3.51	7.01
$[Co(HBMTAAP)_2]$	916.00	60	Brown	196	6.43	62.91	4.88	15.27	3.49	7.02
$[Ni(HBMTAAP)_2]$	915.76	70	Greenish	190	6.41	62.95	4.84	15.29	3.49	7.02
$[Cu(HBMTAAP)_2]$	920.61	55	Green	197	6.90	62.63	4.81	15.20	3.48	6.98
$[Zn(HBMTAAP)_2]$	922.45	68	Yellow	192	7.09	62.46	4.84	15.17	3.47	6.97

In vitro Antibacterial and Antifungal Activity

The agar well diffusion method was used to evaluate the antimicrobial properties of the HBMTAAP ligand and its metal complexes against *S. aureus, B. subtilis, E. coli, P. aeruginosa, C. albicans, and S. cerevisiae*.[2-4] Sterile Mueller–Hinton agar (25 mL) was dispensed into 90 mm Petri plates, allowed to set, and inoculated with 0.5 McFarland microbial suspensions (approx.10^8 CFU/mL). Agar wells (6 mm) were filled with 100 µL of each test solution (10 mg/mL in DMSO).[27-29] The plates were incubated at 37 °C for 24 h (bacteria) and 30 °C for 24–48 h (fungi).[12] A calibrated sliding calliper was used to measure zones of inhibition in mm.

RESULTS AND DISCUSSIONS

Study of HBMTAAP and Related Metallic Complexes

The HBMTAAP ligand and metal complexes were formed as colored solids with overall yields that vary from 58 to 81%. The developed products were soluble in standard organic solvents, which include CCl_4, CH_3COCH_3, DMF, and DMSO. The melting temperatures of metal complexes, including ligand, were from 180 to 197 °C, demonstrating that the produced compounds are thermally stable. The elemental (CHNS) analytical findings corresponded well with the predicted percentages, confirming the complexes' proposed ML_2 stoichiometry. In Table 1, the related physicochemical data were compiled.

^{1}H NMR and Mass Spectra

The HBMTAAP ligand's ^{1}H NMR spectra revealed a singlet at δ 2.253 for the methyl protons deshielded due to adjacent aromatic and azomethine groups. Aromatic -NH_2 protons appeared as a singlet at δ 5.104, while aromatic protons were observed as multiplets at δ 6.651-7.702. The singlet found at δ 12.336 was because of the oxime (–OH) proton, while the hydrazone fragment's -NH protons produced two separate singlets at δ 11.145 and δ 10.828, confirming the presence of the azomethine and hydrazide functionalities in the ligand framework. In the mass spectrum, a molecular ion peak is found at m/z 431.16 $[M+H]^+$ and a sodium adduct peak at m/z 453.14 $[M+Na]^+$, consistent with the calculated molecular weight 430.54 g/mol of $C_{23}H_{22}N_6OS$. The NMR and MS data confirm the identity and purity of the ligand.

Electronic spectra and Magnetic Susceptibility Study

The UV–Vis spectrum (Table-2) of HBMTAAP exhibited bands at 211, 250, 307, and 350 nm, assignable to π → π* and n → π* transitions associated with the aromatic, thiocarbonyl and azomethine group of the ligand.[8] Upon complexation, $[Mn(HBMTAAP)_2]$ exhibited additional bands at 421, 522, 673, and 742 nm, assigned to $^6A_{1g} \rightarrow {}^4T_{1g}(G)$, $^6A_{1g} \rightarrow {}^4T_{2g}(G)$, $^6A_{1g} \rightarrow {}^4A_{1g}(G)/{}^4E_g(G)$, and $^6A_{1g} \rightarrow {}^4T_{1g}(P)$, transitions, supporting a high-spin d^5 octahedral geometry (μ_{eff} = 5.90 B.M., calc. 5.92 B.M.).[1,8,17] The $[Fe(HBMTAAP)_2]$ complex showed broad bands at 562 nm corresponding to LMCT and $^5T_{2g} \rightarrow {}^5E_g$ transitions, consistent with a high-spin d^6 octahedral field (μ_{eff} = 5.50 B.M., calc. 4.90 B.M.).[2-4] The $[Co(HBMTAAP)_2]$ showed absorptions at 775, 532, and 421 nm assigned to $^4T_{1g}(F) \rightarrow {}^4T_{1g}(P)$, $^4T_{1g}(F) \rightarrow {}^4A_{2g}(F)$, and $^4T_{1g}(F) \rightarrow {}^4T_{2g}(F)$ transitions, typical of a high-spin octahedral d^7 system (μ_{eff} = 5.08 B.M.,

calc. 3.87 B.M.).[12,16] The [Ni(HBMTAAP)$_2$] exhibited bands at 780, 552, and 400 nm due to $^3A_{2g}(F) \rightarrow {}^3T_{2g}(F)$, $^3A_{2g}(F) \rightarrow {}^3T_{1g}(F)$, and $^3A_{2g}(F) \rightarrow {}^3T_{1g}(P)$ transitions, indicating a high-spin d^8 octahedral geometry (μ_{eff} = 3.29 B.M., calc. 2.83 B.M.).[12,17] The [Cu(HBMTAAP)$_2$] showed bands at 782 and 620 nm, attributed to $^2E_g \rightarrow {}^3T_{2g}$ and LMCT transitions, suggesting a d^9 tetragonally distorted octahedral geometry due to the Jahn–Teller effect (μ_{eff} = 1.91 B.M., calc. 1.73 B.M.).[17-18] The [Zn(HBMTAAP)$_2$] complex displayed only ligand-centred bands at 203, 240, 310, and 353 nm ($\pi \rightarrow \pi^*$, $n \rightarrow \pi^*$), with no d–d transitions, confirming a diamagnetic d^{10} octahedral configuration (μ_{eff} = 0 B.M.).[5,8]

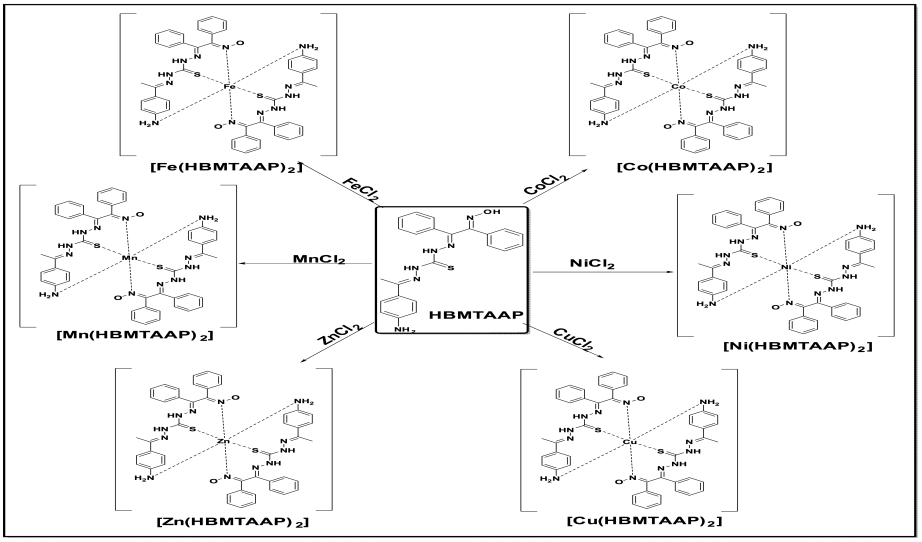

Scheme-2: Synthesis of Transition Metal Complex with HBMTAAP.

Molar Conductivity Measurements

The specific conductance (K) of each metal complex in nitrobenzene (C: 1×10^{-3} mol L^{-1}) was measured at 25 ± 2 °C, and the molar conductance (Λm = K/C) values were calculated.[13] All complexes exhibited conductance values in the range of 1.50-5.39 Ω^{-1} mol^{-1} cm^2, which are significantly lower than the typical values (>50 Ω^{-1} mol^{-1} cm^2) reported for 1:2 electrolytes.[13] The complexes behave as non-electrolytes and do not split into ions in solution, according to the low conductance measurements. This behaviour aligns with the proposed coordination mode, where the oxime (-OH) group participates in chelation, compensating for the divalent metal charge and yielding an electrically neutral ML_2 complex.

FT-IR Spectral Studies

The FT-IR spectrum of HBMTAAP ligand showed a broad peak at 3245 cm^{-1} due to –OH stretching of the oxime and a strong band at 3181 cm^{-1} corresponding to $–NH_2$ and –NH– stretching.[22-23] The azomethine (-C=N-) stretching band appears at 1583 cm^{-1}, while –C=NOH group was detected at 1616 cm^{-1}. [22-25] Aromatic C=C skeletal vibrations are observed at 1516 and 1485 cm^{-1}.[22,25] The stretching at 1220 and 1056 cm^{-1} correspond to >C=S stretching, and at 1026 and 944 cm^{-1} resemble to N–O vibrations.[22-27] Upon complexation, significant spectral changes were observed for -C=N- and -C=S groups, indicating coordination through the nitrogen and sulfur atoms. The oxime –OH band either shifted or showed reduced intensity in the complexes, consistent with deprotonation and coordination through the oxime oxygen. Additionally, changes in the N–O stretching frequency further support metal–oxygen interaction. Overall, the observed spectral shifts confirm that HBMTAAP performs as a tridentate O/N/S donor ligand, directing through aromatic amine N, oxime O, and thiocarbonyl S atoms to form octahedral metal complexes.

Powder XRD Analysis

Powder XRD patterns of the metal complexes were recorded using Cu Kα radiation (λ = 1.5406 Å) across a 2θ scanning range of 10°–80° under uniform experimental conditions.[12] The [Mn(HBMTAAP)$_2$] complex showed weak, broad peaks, indicating an amorphous nature. In contrast, the [Fe(HBMTAAP)$_2$],

$[Co(HBMTAAP)_2]$, $[Ni(HBMTAAP)_2]$, $[Cu(HBMTAAP)_2]$ and $[Zn(HBMTAAP)_2]$ complexes exhibited discernible reflections in the 2θ range of 12°–30°, indicating the presence of crystalline phases. The occurrence of a common reflection near 2θ ~ 20.5° across several complexes suggests a similar structural framework within the series.

Comparative Docking Evaluation Against *PfDHFR*

To evaluate the inhibitory capability of the HBMTAAP ligand, a comparative docking study was conducted using Atovaquone (DB01117) and Proguanil (DB01131), two well-established antimalarial drugs, as reference molecules. Each ligand was docked into the active site of *Plasmodium falciparum dihydrofolate reductase* (*PfDHFR*: 1VDR), and their binding energies and interaction patterns were examined to determine the relative strength and quality of their binding within the active pocket.[34-36] The top-ranked docked poses were illustrated in Fig. 1-3.

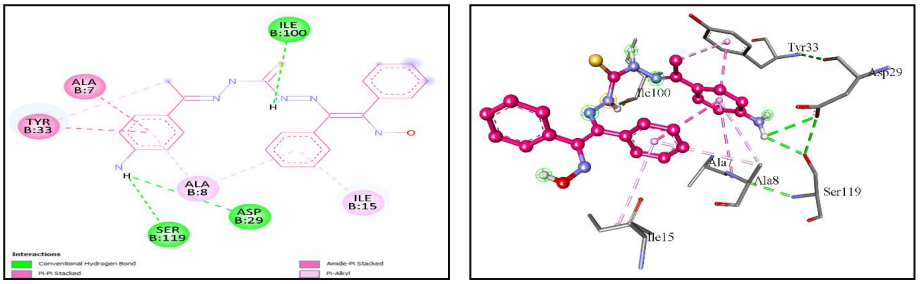

Fig.-1: HBMTAAP 2D and 3D Interactions with *PfDHFR*.

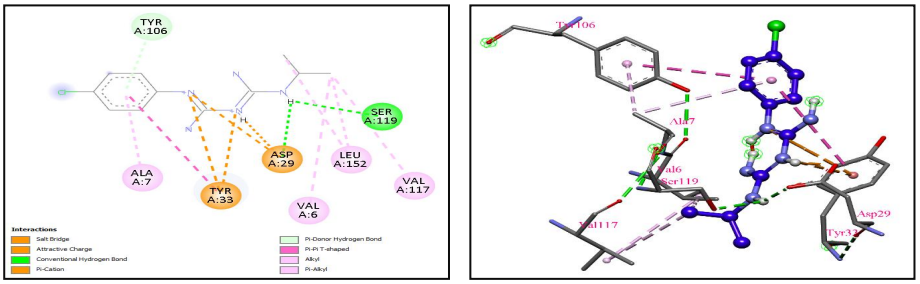

Fig.-2: Proguanil 2D and 3D Interactions with *PfDHFR*.

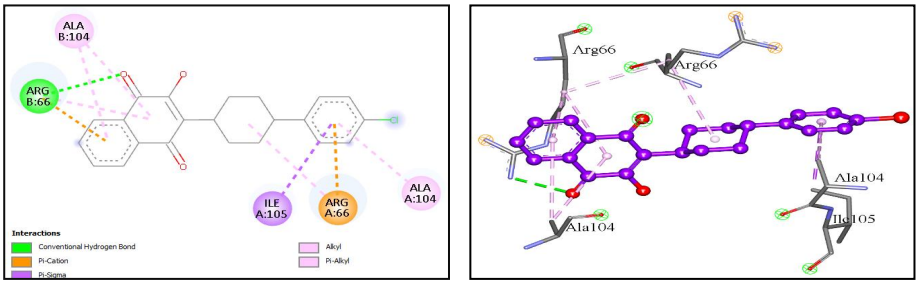

Fig.-3: Atovaquone 2D and 3D Interactions with *PfDHFR*.

Binding Affinity Trends

Among the three compounds, Atovaquone exhibited the highest docking score of –9.9 kcal/mol, consistent with its known high hydrophobic complementarity to *PfDHFR*. The synthesized ligand HBMTAAP demonstrated a comparably strong binding affinity of –9.2 kcal/mol, which closely approaches that of Atovaquone and markedly surpasses the standard antifolate Proguanil (–7.1 kcal/mol). The relatively high binding affinity of HBMTAAP suggests favourable interactions within the catalytic pocket of *PfDHFR*.

Interaction Profile Comparison

Detailed analysis of the binding interactions revealed clear differences in how each ligand engages with the key catalytic residues of *PfDHFR*. The HBMTAAP formed an extensive interaction network,

establishing strong hydrogen bonds with Ser119, Asp29, and Ile100, which contribute to notable electrostatic stabilisation within the active site. The ligand also participated in π–π stacking with Tyr33, amide–π interactions with Tyr8, and several π–alkyl contacts with Ala7, Ala8, and Ile15. The presence of multiple hydrogen bonding and hydrophobic interactions indicates favourable spatial accommodation of HBMTAAP within the *PfDHFR* binding pocket. In contrast, Atovaquone displayed a predominantly hydrophobic binding profile, forming limited hydrogen bonding mainly with Arg66 but showing extensive π–cation and hydrophobic contacts with residues such as Ala104 and Ile105. Proguanil, on the other hand, exhibited comparatively fewer stabilizing interactions, forming hydrogen bonds with Asp29 and Ser119 and showing moderate π-stacking with Tyr33, but with considerably reduced hydrophobic reinforcement relative to both HBMTAAP and Atovaquone.

Overall Comparative Assessment

Overall, the docking results indicate that HBMTAAP forms stable interactions within the *PfDHFR* active site, with binding affinity superior to Proguanil and comparable to Atovaquone. While docking studies provide preliminary insights into binding behaviour, further in vitro and in vivo validation would be required to confirm antimalarial efficacy.

Antibacterial and Antifungal Activities

The agar well diffusion method was applied to examine the antibacterial and antifungal properties of the HBMTAAP ligand and its metal complexes.[2-4] The findings were illustrated in Fig. 4. The free ligand exhibited moderate activity against all evaluated microorganisms, while metal complexation significantly enhanced antimicrobial potency. Among the Gram-positive strains, the [Zn(HBMTAAP)$_2$] complex demonstrated the highest activity, followed by the Co(II) and Ni(II) complexes. For Gram-negative bacteria, the Ni(II) complex demonstrated the strongest inhibition, whereas the Mn(II) complex consistently displayed the weakest activity.

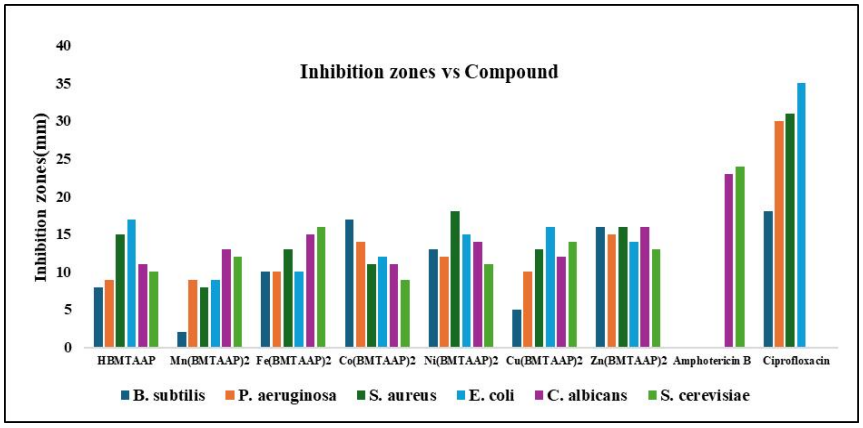

Fig.-4: Biological Activity of HBMTAAP Ligand and its Metal Complexes.

A similar trend was observed in antifungal screening, where the Fe(II), Zn(II), and Mn(II) complexes showed enhanced inhibition in contrast to the HBMTAAP ligand. The observed enhancement in biological activity upon complex formation is explained by Tweedy's Chelation Theory, which states that chelation reduces the polarity of the metal ion through partial sharing of electrons with donor atoms.[33] The result improves the lipophilicity of the complex, improving its permeation via microbial cell membranes, resulting in improved antimicrobial efficacy. Overall, the outcomes show that metal coordination considerably increases the biological potential for the HBMTAAP ligand.

CONCLUSION

The HBMTAAP ligand and its first-row transition metal complexes were effectively produced and structurally investigated. Spectroscopic, magnetic, and conductivity studies confirmed the formation of neutral ML_2 complexes with predominantly octahedral geometry and tridentate O/N/S coordination. Antimicrobial evaluation demonstrated enhanced activity upon metal coordination, consistent with

chelation theory. Molecular docking of the free ligand against *Plasmodium falciparum dihydrofolate reductase* (*PfDHFR*) revealed favourable binding interactions, indicating potential antimalarial relevance. These findings highlight the significance of metal coordination in modulating microbial activity and assist in the development of new antimicrobial strategies aligned with Sustainable Development Goal 3 (Good Health and Well-being). Further investigations, including minimum inhibitory concentration (MIC) determination, cytotoxicity evaluation, in vitro antimalarial assays, and mechanistic studies, are required to validate the biological potential of this ligand system and its metal complexes.

ACKNOWLEDGMENTS

The Authors are thankful to Platinum Industries Limited, Palghar, Maharashtra (401404), India, and Riva Industries, 289/ Kirwali, Raigad, Maharashtra (410201), India, for their valuable support and assistance during this research work.

CONFLICT OF INTERESTS

The authors declare that they have no conflicts of interest.

AUTHOR CONTRIBUTIONS

The present work is related to *SDG-3: Good Health and Well-being*. All the authors contributed significantly to this manuscript, participated in reviewing/editing and approved the final draft for publication. The research profile of the authors can be verified from their ORCID ids, given below:

Digvijay Zarekar https://orcid.org/0009-0003-1133-0515
Raj Badekar https://orcid.org/0000-0002-9425-4743
Gourishanker Jha https://orcid.org/0009-0004-1644-7795
Roshani Gupta https://orcid.org/0009-0009-8725-2393
Sandesh Jaybhaye https://orcid.org/0000-0001-7826-4995

Cite this article as: D. B. Zarekar *et al.*, *Rasayan J. Chem.*, 19(2), 858-865(2026), https://doi.org/10.31788/RJC.2026.1929661.

REFERENCES

1. A. Z. El-Sonbati, W. H. Mahmoud, G. G. Mohamed, M. A. Diab, S. M. Morgan, and S. Y. Abbas, *Applied Organometallic Chemistry*, **33**, e5048(2019), https://doi.org/10.1002/aoc.5048
2. D. B. Pallai, R. R. Badekar, K. I. Momin, A. S. Bondge, G. R. Nagargoje, P. D. Kadam, S. P. Panchgalle, and V. S. More, *Journal of Applied Organometallic Chemistry*, **4**, 76(2024), https://doi.org/10.48309/jaoc.2024.434283.1156
3. D. Pallai, M. D. Dsouza, K. I. Momin, A. S. Bondge, D. D. Kadam, P. P. Bhujbal, G. R. Nagargoje, P. D. Kadam, S. P. Panchgalle, and V. S. More, *Oriental Journal of Chemistry,* **40**, 806(2024), http://doi.org/10.13005/ojc/400324
4. D. Zarekar, G. Jha, S. Hawaldar, R. Gupta, S. Jaybhaye, *African Journal of Biomedical Research,* **27**, 534(2024), https://doi.org/10.53555/AJBR.v27i1.9041
5. M. Yadav, S. Sharma, J. Devi, *Journal of Chemical Sciences*, **133**, 21(2021), https://doi.org/10.1007/s12039-020-01854-6
6. N. P. Singh, K. Kumar, A. Kumar, and U. Agarwal, *Rasayan Journal of Chemistry*, **13**, 215(2020), http://doi.org/10.31788/RJC.2020.1315571
7. S. M. Abd El-Hamid, S. A. Sadeek, S. F. Mohammed, F. M. Ahmed, and M. S. El-Gedamy, *Applied Organometallic Chemistry*, **37**, e6958(2023), https://doi.org/10.1002/aoc.6958
8. T. A. Alorini, A. N. Al-Hakimi, S. El-Sayed Saeed, E. H. L. Alhamzi, and A. E. Albadri, *Arabian Journal of Chemistry*, **15,** 103559(2022), https://doi.org/10.1016/j.arabjc.2021.103559
9. G. S. Kondareddy, H. S. Kengunte, and R. A. Medehal, *Rasayan Journal of Chemistry*, **14**, 2246(2021), http://doi.org/10.31788/RJC.2021.1446507
10. P. Yadav, R. Badekar, P. Nag, and R. Lokhande, *Journal of Advanced Scientific Research*, **12**, 231(2021), https://doi.org/10.55218/JASR.202112130

11. K. Sirumalar, M. Paul Johnpeter, R. Manikandan, A. P. Mary Sri Archana, and A. Paulraj, *Rasayan Journal of Chemistry*, **14**, 1316(2021), http://doi.org/10.31788/RJC.2021.1426283
12. W. H. Mahmoud, and R. G. Deghadi, *Applied Organometallic Chemistry,* **32**, e4289(2018), https://doi.org/10.1002/aoc.4289
13. I. Ali, W. A. Wani, and K. Saleem, *Synthesis and Reactivity in Inorganic, Metal-Organic, and Nano-Metal Chemistry*, **43**, 1162(2013), https://doi.org/10.1080/15533174.2012.756898
14. R. Vindhya, T. M. Sharanakumar, Veerendra Kumar A. Kalalbandi, K. N. Shashiraj, K. M. Nagarsha, H. M. Suresh Babu, and Suresh, *Rasayan Journal of Chemistry*, **17**, 945(2024), http://doi.org/10.31788/RJC.2024.1738886
15. M. Orojloo, P. Zolgharnein, M. Solimannejad, and S. Amani, *Inorganica Chimica Acta*, **467**, 227(2017), https://doi.org/10.1016/j.ica.2017.08.016
16. J. Titis, J. Hudak, J. Kozisek, A. Krutosikova, J. Moncol, D. Tarabova, and R. Boca, *Inorganica Chimica Acta*, **388**, 106(2012), https://doi.org/10.1016/j.ica.2012.03.036
17. W. H. Mahmoud, G. G. Mohamed, and O. Y. El-Sayed, *Applied Organometallic Chemistry,* **32**, e4051(2018), https://doi.org/10.1002/aoc.4386
18. L. H. Abdel-Rahman, A. M. Abu-Dief, H. Moustafa, and S. K. Hamdan, *Applied Organometallic Chemistry*, **31**, e3555(2017), https://doi.org/10.1002/aoc.3555
19. M. Abdul-Salam, and N. A. Tawfeeq, *International Journal of Health Sciences*, **6**, 10419(2022), https://doi.org/10.53730/ijhs.v6nS4.12208
20. B. S. Furniss, A. J. Hannaford, P. W. G. Smith, and A. R. Tatchell, Vogel's Textbook of Practical Organic Chemistry, 5th Ed., Longman Scientific & Technical, London, p.**1048**(1989)
21. J. Wazir, *International Journal of Medical Works Online,* **1**, 5(2015), https://doi.org/10.5281/zenodo.160807
22. R. A. Bedier, T. A. Yousef, G. M. Abu El-Reash, and O. A. El-Gammal, *Journal of Molecular Structure*, **1139**, 436(2017), https://doi.org/10.1016/j.molstruc.2017.03.054
23. V. K. Sharma, and S. Srivastava, *Journal of Coordination Chemistry*, **61**, 178(2008), https://doi.org/10.1080/00958970701318426
24. M. S. Surendra Babu, T. B. Patrudu, and K. Hussain Reddy, *E-Journal of Chemistry*, **8**, S309(2011), https://doi.org/10.1155/2011/567979
25. K. Gangarapu, S. Manda, A. Jallapally, S. Thota, S. S. Karki, J. Balzarini, D. E. Clercq, and H. Tokuda, *Medicinal Chemistry Research*, **23**, 1046(2014), https://doi.org/10.1007/s00044-013-0684-3
26. J. Zhou, D. Wu, and D. Guo, *Journal of Chemical Technology and Biotechnology*, **85**, 1402(2010), https://doi.org/10.1002/jctb.2446
27. A. A. Al-Shamry, M. M. Khalaf, H. M. A. El-Lateef, T. A. Yousef, G. G. Mohamed, K. M. K. El-Deen, M. Gouda, and A. M. Abu-Dief, *Materials*, **16**, 83(2023), https://doi.org/10.3390/ma16010083
28. S. Wagh, B. R. Patil, *Rasayan Journal of Chemistry,* **15**, 1718(2022), http://doi.org/10.31788/RJC.2022.1536355
29. D. Dehari, A. Chaudhuri, D. N. Kumar, R. Patil, M. Gangwar, S. Rastogi, D. Kumar, G. Nath, and A. K. Agrawal, *Pharmaceuticals*, **16**, 942(2023), https://doi.org/10.3390/ph16070942
30. T. Gupta, *Sciencia Acta Xaveriana*, **6**, 1(2015)
31. O. M. Hilal, and G. E. Fredericks, *Journal of the Chemical Society*, 785(1954), https://doi.org/10.1039/JR9540000785
32. D. Skalamera, E. Sanders, R. Vianello, A. Marsavelski, A. Pevec, I. Turel, and S. Kirin, *Dalton Transactions*, **45**, 2845(2015), https://doi.org/10.1039/C5DT03387J
33. B. G. Tweedy, *Phytopathology*, **55**, 910(1964).
34. L. Yang, Y. Xiaocong, G. Jianhong, C. Shuang, X. Zhi-Xiong, and C. Yang, *Nucleic Acids Research*, **50**, 159(2022), https://doi.org/10.1093/nar/gkac394
35. Y. Xiaocong, L. Yang, G. Jianhong, X. Zhi-Xiong, and C. Yang, *Briefings in Bioinformatics*, **23**, bbac087, (2022), https://doi.org/10.1093/bib/bbac087
36. U. Pieper, O. Herzberg, G. Kapadia, M. Mevarech, and O. Herzberg, *Structure,* **6**, 75(1998), https://doi.org/10.1016/S0969-2126(98)00009-4

[RJC-9661/2026]